

Wnt7b regulates mesenchymal proliferation and vascular development in the lung

Weiguo Shu, Yue Qin Jiang, Min Min Lu and Edward E. Morrisey*

Department of Medicine and the Molecular Cardiology Research Center, University of Pennsylvania, Philadelphia, PA 19104, USA

*Author for correspondence (e-mail: emorrise@mail.med.upenn.edu)

Accepted 17 July 2002

SUMMARY

Although the Wnt signaling pathway regulates inductive interactions between epithelial and mesenchymal cells, little is known of the role that this pathway plays during lung development. Wnt7b is expressed in the airway epithelium, suggesting a possible role for Wnt-mediated signaling in the regulation of lung development. To test this hypothesis, we have mutated Wnt7b in the germline of mice by replacement of the first exon with the *lacZ*-coding region. *Wnt7b^{lacZ-/-}* mice exhibit perinatal death due to respiratory failure. Defects in early mesenchymal proliferation leading to lung hypoplasia are observed in

Wnt7b^{lacZ-/-} embryos. In addition, *Wnt7b^{lacZ-/-}* embryos and newborn mice exhibit severe defects in the smooth muscle component of the major pulmonary vessels. These defects lead to rupture of the major vessels and hemorrhage in the lungs after birth. These results demonstrate that Wnt7b signaling is required for proper lung mesenchymal growth and vascular development.

Key words: Wnt7b, Lung, Mesenchyme, Proliferation, Vascular smooth muscle

INTRODUCTION

Proper lung development is essential for postnatal survival, and pulmonary defects are a leading cause of neonatal illness and mortality in humans (Guyer et al., 1999). Development of the mouse lung closely parallels that of the human lung and as such provides a powerful model in which to study lung development. Formation of the mouse lung begins at ~E9.5 of development by budding from the foregut endoderm. This early lung endoderm, which is surrounded by mesodermally derived mesenchyme, undergoes branching morphogenesis to produce the three-dimensional arborized network of airways required for postnatal respiration in mammals (Warburton et al., 2000). During branching morphogenesis, the pulmonary mesenchyme gives rise to several different cell types, including smooth muscle of the upper airways and the pulmonary vasculature. In addition, the mesenchyme produces essential growth factors and signaling molecules required for airway epithelial development and branching including members of the fibroblast growth factor (FGF) family (reviewed by Warburton et al., 2000). In turn, the epithelium also produces signaling molecules important for mesenchymal differentiation and proliferation including bone morphogenetic protein 4 (BMP4) and sonic hedgehog (SHH) (Bellusci et al., 1997; Bellusci et al., 1996; Litingtung et al., 1998; Pepicelli et al., 1998). Therefore, the inductive interactions between mesenchyme and epithelium are crucial to the generation and patterning of the mammalian lung.

Like several other organ systems, the lung is patterned in a

proximodistal manner. Proliferation in airway epithelium occurs at a higher level in distal versus proximal regions during development (Hogan and Yingling, 1998; Warburton et al., 2000). Distinct epithelial cell lineages arise from the common epithelial precursor cells to generate the necessary cell types for adult respiration including alveolar epithelial type 1 (AEC-1) and type 2 (AEC-2) cells. AEC-1 cells themselves are thought to differentiate from AEC-2 cells through an as yet uncharacterized mechanism (Evans et al., 1975). AEC-1 and AEC-2 cells are found only in the distal airway epithelium during development. AEC-1 cells are required to form the thin, diffusible stratum between the airway lumen and the pulmonary capillary network, whereas AEC-2 cells produce surfactant to maintain the proper airway surface tension for respiration. In addition, defects in surfactant protein expression cause neonatal distress and death in humans (Ballard, 1996; Noguee et al., 1994). As the airway epithelium develops proximally, cell types such as Clara epithelial cells and ciliated epithelium of the upper airways become the primary cell types populating this region of the lung. The proper proximodistal differentiation of the airway epithelium is essential for proper lung development, as shown by the neonatal lethality of mice expressing the BMP inhibitors noggin and gremlin, which disrupt proximodistal patterning (Lu et al., 2001; Weaver et al., 1999). Thus, this patterning in the lung results in the establishment of a large, functional airway surface area that is capable of efficiently exchanging gases with the environment and expelling inhaled particulate matter.

The lung mesenchyme is also patterned in a proximodistal

manner. This is exemplified by the recruitment of smooth muscle surrounding the proximal airways and proximal blood vessels and not the distal airways and blood vessels. This patterning is closely linked to that observed in the epithelium as blocking BMP signaling in a distal epithelial cell autonomous manner results in the disruption of proximodistal patterning of both the epithelium and mesenchyme, including the ectopic appearance of smooth muscle surrounding the distal airways (Weaver et al., 1999). Thus, the proper level of proliferation and differentiation along a proximodistal axis is necessary for several aspects of lung development; the elucidation of the signals involved in these processes will provide important insights into embryonic lung development.

The Wnt growth factor family is comprised of at least 18 different secreted ligands that interact with 10 known frizzled receptors. Wnt signals are key regulators of cell proliferation, polarity and differentiation (reviewed by Cadigan and Nusse, 1997; Wodarz and Nusse, 1998). Wnts signal through multiple pathways, the best studied of these being the β -catenin/LEF-TCF pathway also known as the canonical pathway (Parr and McMahon, 1994; Willert and Nusse, 1998). In this pathway, secreted Wnt proteins bind to the cell membrane receptors of the frizzled family, inhibiting GSK-3 β -mediated phosphorylation of β -catenin. Hypophosphorylated β -catenin accumulates in the cytoplasm and is translocated to the nucleus where it heterodimerizes with members of the LEF/TCF transcription factor family. A role for Wnt signaling in lung development is suggested by the observation that several Wnt genes are expressed in the developing lung mesenchyme and/or epithelium. In particular, *Wnt7b* is expressed at high levels in distal airway epithelium (Pepicelli et al., 1998; Weidenfeld et al., 2002). However, the functions of *Wnt7b* and the Wnt signaling pathway in lung development are unknown.

To determine the role that *Wnt7b* plays during development, we generated mice bearing a mutant *Wnt7b* allele in which the *lacZ*-coding region replaces the coding region of the first exon. *Wnt7b^{lacZ}* mice die perinatally due to respiratory failure. The lungs of *Wnt7b^{lacZ}* mice do not inflate, are hypoplastic and show extensive hemorrhage at birth. Lung hypoplasia in *Wnt7b^{lacZ}* embryos is evident as early as E12.5 of development and is due, at least in part, to decreased cell proliferation in the distal mesenchyme adjacent to the growing tips of the distal airway epithelium where *Wnt7b* is normally expressed. *Wnt7b^{lacZ}* embryos also exhibit defects in late airway epithelial maturation. Histological analysis of *Wnt7b^{lacZ}* neonatal mice and embryos reveals that vascular smooth muscle is hypertrophic and, at birth, apoptotic, which leads to vessel rupture and hemorrhage. These results demonstrate that *Wnt7b* signaling is necessary for proliferation and growth of the lung mesenchyme and for maturation of the airway epithelium.

MATERIALS AND METHODS

Generation of *Wnt7b^{lacZ}* mice

Wnt7b mouse BAC clones were obtained from a commercial source (Incyte, Palo Alto, CA). Southern blotting and PCR were used to map the mouse *Wnt7b* gene. PCR was used to generate 3.5 kb of 5' flanking region which includes the *Wnt7b* 5' untranslated sequence but lacks the endogenous *Wnt7b* initiating ATG. This fragment was fused to the

coding sequence of the bacterial *lacZ* sequence followed by a SV40 poly(A) sequence (Zhang et al., 2001). A 6.5 kb 3' *Bam*HI fragment was cloned into the *Bam*HI site of pPNT and the 7.5 kb 5' arm/*lacZ*-coding sequence was cloned into the *NotI/XhoI* sites of pPNT to generate the p*Wnt7b/lacZ*-KO vector. This targeting vector was linearized with *NotI* and electroporated into R1 ES cells, which were selected in 250 μ g/ml G418 and 0.2 μ M FIAU for 8 days at which time resistant clones were picked and analyzed by Southern blotting for identification of homologous recombinants. Two correctly targeted clones were injected into C57BL/6 E3.5 blastocysts and chimeric mice from each clone were mated for germline transmission of the allele. The phenotype was identical for animals derived from both ES clones on a 129SVJ background or 129SVJ-C57BL/6 mixed background.

RT-PCR and co-transfection assays

For RT-PCR, total RNA was extracted from wild-type and *Wnt7b^{lacZ}* E14.5 lung tissue using Trizol. Two micrograms of RNA was subjected to reverse transcriptase-cDNA synthesis using the Superscript II enzyme (Gibco-BRLc). Ten percent of each RT reaction was then subjected to PCR using the following cycling conditions:

short distance – 94°C for 20 seconds, 65°C for 1 minute, 72°C for 1 minute, 35 cycles;

long distance – 98°C for 20 seconds, 68°C for 6 minutes.

For short distance PCR, the Takara Ex Taq enzyme was used, while for the long distance PCR, the Takara La Taq enzyme was used (Panvera, Madison, WI). The oligos used for these reactions are as follows: A, 5'-GGGCTCACCATTGGTGGCAACGCG-3'; B, 5'-GGGATCTGCCATTGTCAGACATG-3'; C, 5'-AACTGGTGCTGGCACTCGTCG-3'; D, 5'-CGCATGCTGTCACCGTGCCTGC-3'; E, 5'-CCGAATTCAGACCACCATTGCGTTGAC-3'; GAPDH, 5' 5'-GAGTCTACTGGTGTCTTACCACC-3'; and GAPDH, 3' 5'-CGCAGGAGACAACCTGGTCTCAG-3'.

To generate the full-length *Wnt7b* and truncated *Wnt7b* cDNA expression vectors, *Wnt7b* was amplified from mouse embryonic lung cDNA using the following oligonucleotides: *Wnt7b*, 5' full-length 5'-CACGAATTCGAGATGCACAGAACTTTCGAAAGTGG-3'; *Wnt7b*, 5' truncated 5'-CACGAATTCCTCGGAGCATTGTCATC-CGTGGTG-3'; *Wnt7b*, 3' 5'-CACTCTAGATCACTTGCAGGTGAA-GACCTCGGTGCGCTC-3'. The amplified products were cloned into the pcDNA3 vector. An HA epitope tag was incorporated at the 3' end of each cDNA. HEK-293 cells were transfected with these expression constructs using Fugene 6 (Roche Biochemicals). After 48 hours, cells were stained with a monoclonal antibody to the HA epitope (HA.11, Convince) and analyzed by fluorescent microscopy.

Histological procedures

For in situ hybridization, embryos were fixed in 4% paraformaldehyde for 24–48 hours, depending on age. Fixed embryos were dehydrated through increasing ethanol concentrations and embedded in paraffin wax. Sections (5 μ m) were used for radioactive in situ hybridization as well as immunohistochemistry. The aquaporin-5, SP-C, CC10, SHH probes have been previously described (Lu et al., 2001; Pepicelli et al., 1998). In situ hybridization was performed using a previously published protocol (Kuo et al., 1997). β -gal staining was performed as previously described (Kim et al., 1997). Further details on histological protocols can be found at the Molecular Cardiology Research Center (<http://www.uphs.upenn.edu/mcrc/histology/histologyhome.html>).

Cell proliferation assays

Immunohistochemistry using a phospho-histone H3 monoclonal antibody was used to detect mitotic cells (clone 6G3, Cell Signaling Technology) (Hans and Dimitrov, 2001; Saka and Smith, 2001). Briefly, sections from paraformaldehyde fixed E14.5 wild-type and *Wnt7b^{lacZ}* embryos were probed with the phospho-histone H3 monoclonal antibody at a 1:250 dilution overnight at room temperature. Slides were washed and then probed with rabbit anti-

mouse HRP antibody at a 1:100 dilution. After a final set of washes, slides were developed using a commercially available kit (Vector Laboratories). Slides were counterstained with Hematoxylin. Positive cells, as well as the total cell number, were counted in an approximately 60° radius of growing epithelial tubules in three adjacent slides from four different embryos of each indicated genotype using the NIH Image 1.62 software.

Cardiac acrylic resin injections for visualizing vascular abnormalities

To visualize the pulmonary vascular defects in *Wnt7b^{lacZ}* embryos, Batson 17 acrylic resin (Polysciences, Warrington, PA) was injected into the ventricles of the heart of E18.5 *Wnt7b^{lacZ}* and wild-type littermates until the embryonic vasculature was filled. After hardening, soft tissue was digested with maceration solution (Polysciences, Inc.) at 37°C for 3 days. Photographs of lung vascular network casts were taken on a Leica Model MZ125 dissecting microscope with a Leica digital camera.

RESULTS

Generation of a *Wnt7b^{lacZ}* mutant mouse

The coding sequences of the first exon of mouse *Wnt7b* were replaced with the coding sequence of the *lacZ* gene by homologous recombination in embryonic stem cells (Fig. 1A). The resulting *Wnt7b* gene lacks the endogenous ATG initiation codon as well as the predicted signal peptide

sequence, which should eliminate the ability of *Wnt7b* to be secreted (Nielsen et al., 1997). This strategy was employed because previous experiments have shown that the signal peptide sequence is required for Wnt activity in *Xenopus* embryos and cell culture (Mason et al., 1992; McMahon and Moon, 1989). Germline transmission of the targeted allele was confirmed by Southern blotting of genomic DNA using the indicated probe (Fig. 1B).

RT-PCR was used with RNA from E14.5 *Wnt7b^{+/+}* and *Wnt7b^{-/-}* embryonic lungs to detect possible spliced products in the 3' region of the *Wnt7b* gene as well as splicing that could occur from either the 5'UTR or the *lacZ* sequences to the 3' region. As shown in Fig. 1C, we do not detect any spliced products stemming from the 5' first exon or from the *lacZ* sequences either by standard PCR or by long distance PCR (Fig. 1C and data not shown). However, transcripts were detected that contained both exon 3 and 4 in the *Wnt7b^{lacZ}* lung RNA, albeit at markedly lower levels than in wild-type animals (Fig. 1C). This raised the possibility that a truncated *Wnt7b* protein could be produced from the *Wnt7b^{lacZ}* allele. HEK-293 cells were transfected with either a full-length *Wnt7b* expression construct or a construct that contained a *Wnt7b* cDNA that lacked the sequence transcribed by the first exon that are deleted in *Wnt7b^{lacZ}* mice to determine whether the potential truncated *Wnt7b* cDNA would produce a stable, secreted protein. Using an antibody against the hemagglutinin

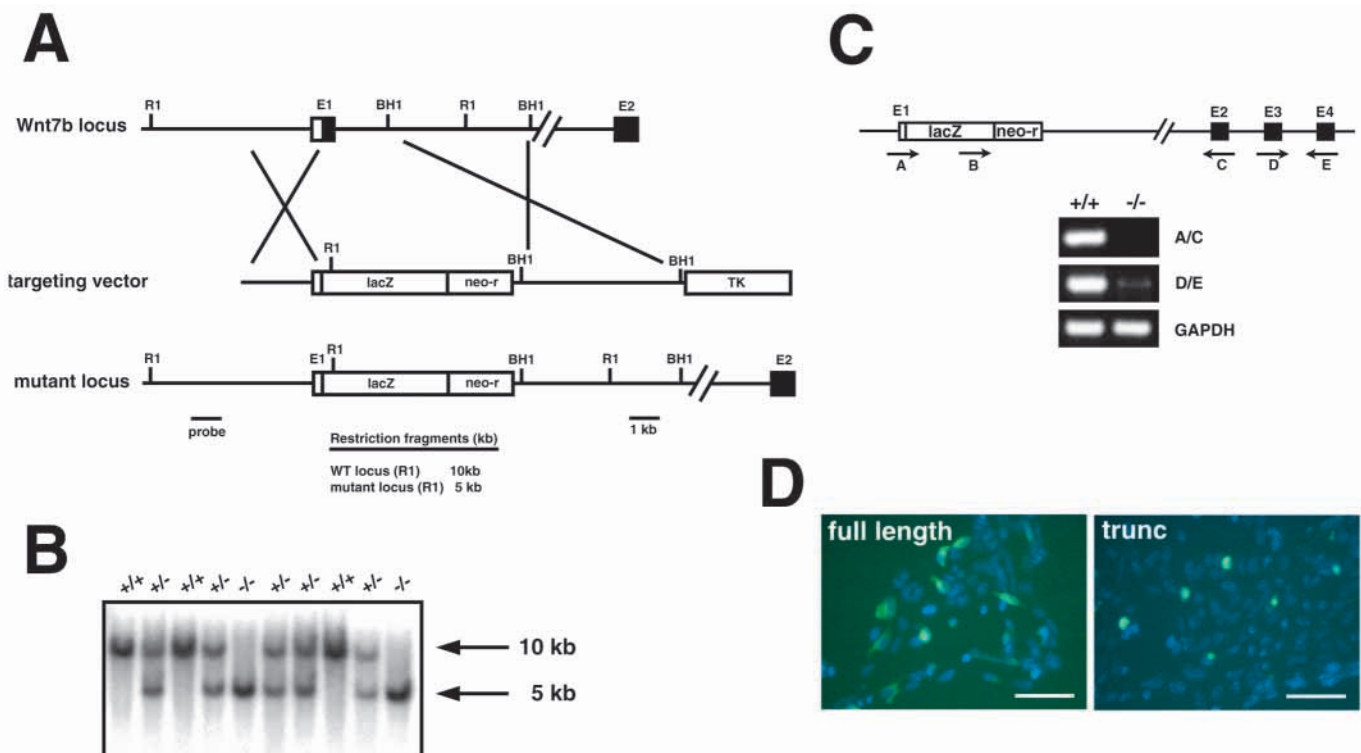


Fig. 1. Targeting strategy for generation of the *Wnt7b^{lacZ}* mice. (A) Schematic of *Wnt7b* targeting construct. (B) Southern blot of a litter of newborn mice indicating the wild-type allele (10 kb) and the mutant allele (5 kb), resulting from an *EcoRI* restriction enzyme digest. (C) RT-PCR analysis of mRNA from E14.5 mouse lungs from *Wnt7b^{lacZ}* embryos. The *Wnt7b^{lacZ}* targeted allele and the oligonucleotide used for RT-PCR are shown. No amplifiable transcripts were obtained using oligo combinations A/C or A/E (data not shown) from *Wnt7b^{lacZ}* embryos while wild-type (+/+) mRNA produced a robust signal. Low levels of transcript were obtained using oligos D and E with lung cDNA from *Wnt7b^{lacZ}* embryos. (D) HEK-293 cells were transfected with either HA-tagged full-length or truncated (trunc) *Wnt7b* cDNAs. The truncated *Wnt7b* cDNA represented the complete coding region from the last three exons, which are still present in the *Wnt7b^{lacZ}* allele. Cells are counterstained with DAPI to visualize the nucleus. Scale bar: 40 μ m.

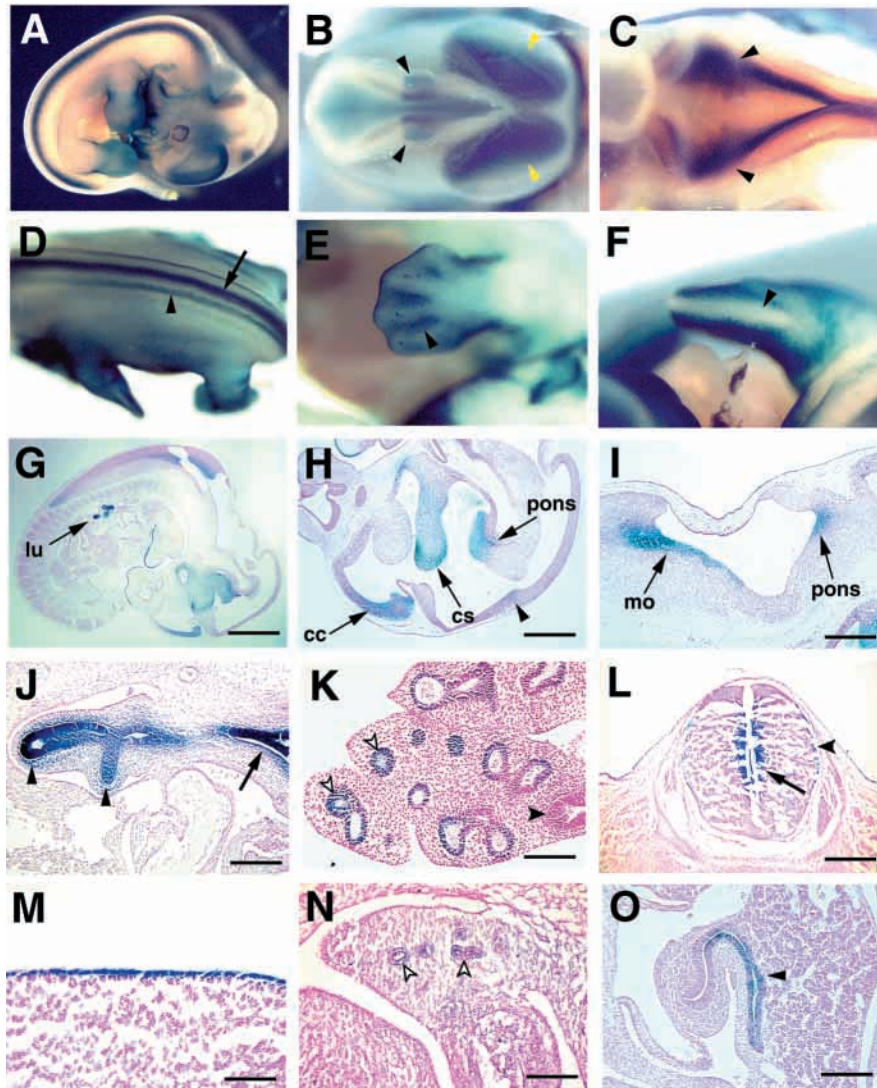


Fig. 2. The *Wnt7b^{lacZ}* allele recapitulates endogenous *Wnt7b* expression. *lacZ* staining of E12.5 (A–J, L, N, O) and E14.5 (K, M) embryos reveals that the *Wnt7b^{lacZ}* allele drives expression of the *lacZ* gene in a pattern identical to the endogenous mouse *Wnt7b* gene. β -galactosidase expression is observed in the future cerebral cortex (B, yellow arrowhead), in a narrow band across the roof of the midbrain (B, black arrowhead) and the medulla oblongata (C, arrowheads). Histological sections of E12.5 embryos reveals expression in the ependymal (D, L, arrow) and the outer marginal layers (D, L, arrowhead) of the neural tube and the corpus striatum (cs), pons (pons) and the medulla oblongata (mo) (H, I). β -galactosidase expression is observed in the interdigital mesenchyme of the forming limb bud (E, arrowhead) but is excluded from the apical ridge (F, arrowhead). High levels of β -galactosidase expression are observed in the developing lung (G, lu) and trachea, and are restricted to the airway epithelium (J, arrowheads indicate lung epithelium, arrow indicates trachea; K, arrowheads). By E14.5, expression in the airway epithelium is restricted to the distal regions (K, compare white arrowheads with black arrowhead). β -Galactosidase expression is observed in the developing skin at E14.5 (M), in the metanephric tubules of the developing kidney (N, arrowheads), and in the epithelium of the bile duct (O, arrowhead). Scale bars: 1.5 mm in G; 750 μ m in H; 500 μ m in I; 350 μ m in J; 250 μ m in K, L, O; 125 μ m in N; 75 μ m in M.

(HA) epitope, transfected cells were stained for the cellular localization of the full length and truncated *Wnt7b* proteins. The full length *Wnt7b* protein was located throughout the cytoplasm and cell periphery (Fig. 1D). However, the truncated *Wnt7b* protein was localized in a perinuclear pattern reminiscent of the endoplasmic reticulum (ER) (Fig. 1D). Retention of proteins in the ER is thought to result from improper folding and subsequent degradation of mutant protein products (Lippincott-Schwartz et al., 1988). These data indicate that although the *Wnt7b^{lacZ}* allele produces low levels of transcripts at the 3' end of the gene, any resulting protein made from this transcript is not likely to be stable or secreted.

The *Wnt7b^{lacZ}* allele recapitulates the endogenous pattern of mouse *Wnt7b* expression

The substitution of the first exon with the coding sequences of the *lacZ* gene in the *Wnt7b^{lacZ}* allele allowed us to carry out a detailed examination of the expression pattern of *Wnt7b* during development. Previous reports using in situ hybridization have shown that *Wnt7b* is expressed in the airway epithelium of the lung, proximal tubules of the

forming kidney, the spinal cord and the brain (Hollyday et al., 1995; Parr et al., 1993; Pepicelli et al., 1998; Rubenstein et al., 1999; Weidenfeld et al., 2002). Staining of E12.5–E14.5 embryos for β -galactosidase expression shows that our *Wnt7b^{lacZ}* allele accurately recapitulates the endogenous expression pattern (Fig. 2A). *Wnt7b^{lacZ}* expression is observed in the frontal edge of the future cerebral cortex as well as in a thin streak across the roof of the midbrain (Fig. 2B, H). In the developing spinal cord, the *Wnt7b^{lacZ}* allele is expressed in the ependymal and the outer marginal layers (Fig. 2D, L). In the limb bud, β -galactosidase expression is observed in the interdigital mesenchyme but is excluded from the apical ridge (Fig. 2E, F). In the lung, β -galactosidase is observed at high levels in the distal airway and tracheal epithelium, while in the kidney, expression is observed in the metanephric tubules (Fig. 2G, J, K, N). Expression of the *Wnt7b^{lacZ}* allele is also observed in the developing skin and in the developing bile duct, which has not been previously reported (Fig. 2M, O). These data suggest that the *Wnt7b^{lacZ}* allele recapitulates the endogenous expression of the mouse *Wnt7b* gene and further indicates that the gene has been correctly targeted. In addition, these data reveal previously

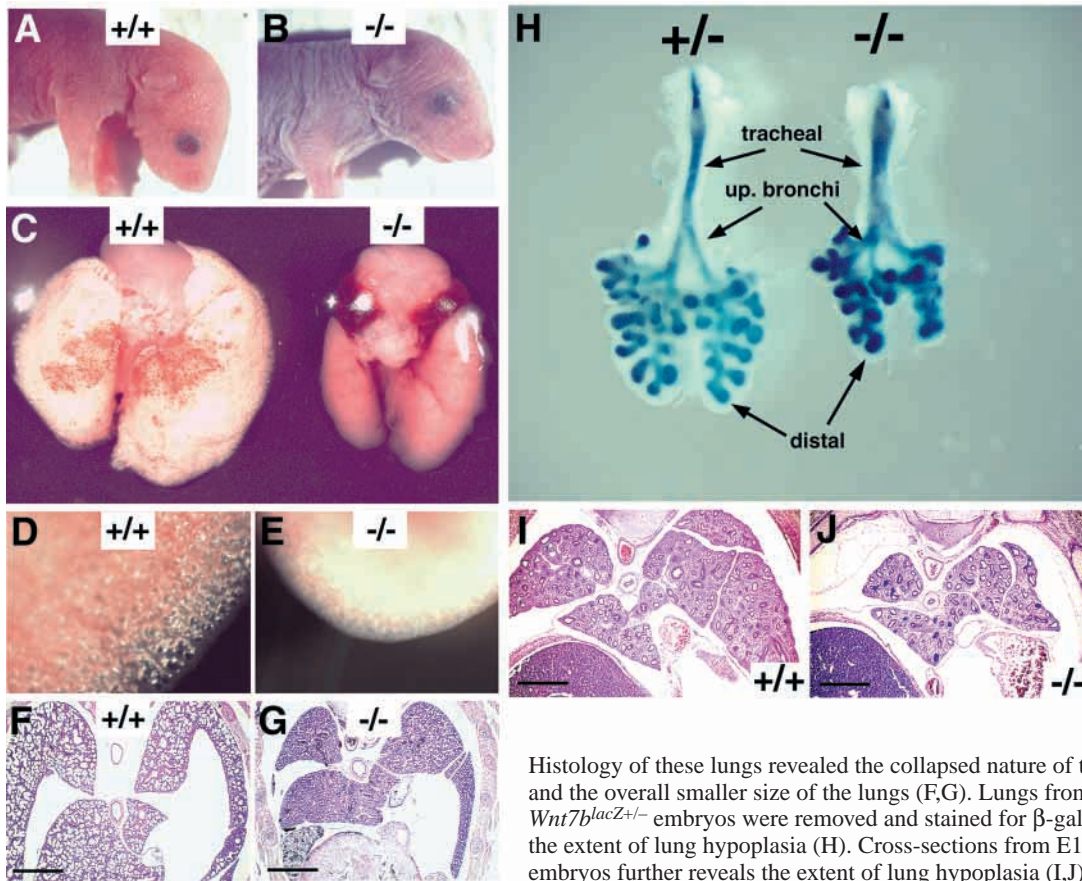


Fig. 3. *Wnt7b^{lacZ-/-}* neonates die quickly after birth, because of respiratory distress, and display lung hypoplasia. Examination of neonates during birth revealed that a population of them did not turn pink but were cyanotic and gasped for air, quickly succumbing within minutes (A versus B). Examination of wild-type lungs showed that they were expanded by inhalation of air (C), which can be observed as air bubbles in the distal regions of the lung (D). The *Wnt7b^{lacZ-/-}* lungs were collapsed and hypoplastic, lacking visible air in the lung periphery (E).

Histology of these lungs revealed the collapsed nature of the airways in *Wnt7b^{lacZ-/-}* mice and the overall smaller size of the lungs (F,G). Lungs from E12.5 *Wnt7b^{lacZ-/-}* and *Wnt7b^{lacZ+/+}* embryos were removed and stained for β -galactosidase expression to reveal the extent of lung hypoplasia (H). Cross-sections from E14.5 wild-type and *Wnt7b^{lacZ-/-}* embryos further reveals the extent of lung hypoplasia (I,J).

unknown regions of *Wnt7b* expression such as in the developing bile duct.

Wnt7b^{lacZ-/-} mice die quickly after birth due to respiratory failure

Wnt7b^{lacZ+/+} mice were mated to produce *Wnt7b^{lacZ-/-}* offspring. Eighty-five 2-week-old mice from *Wnt7b^{lacZ+/+}* crosses were genotyped and no live homozygous null mice were found (Table 1). We then determined the time of death of *Wnt7b^{lacZ-/-}* mice. The expected Mendelian ratio was obtained at all embryonic time points, including immediately post-delivery (Table 1). However, examination of newborn pups revealed that approximately 25% of them gasped for breath, appeared cyanotic and died within 10 minutes of delivery (Fig. 3A,B). In all cases, pups that died within minutes of birth were genotyped as *Wnt7b^{lacZ-/-}* mice. When compared with the lungs of wild-type littermates, the lungs of *Wnt7b^{lacZ-/-}* neonatal mice were significantly smaller in appearance (Fig. 3C). In addition, lungs of *Wnt7b^{lacZ-/-}* mice did not show

evidence of air in the distal airways (Fig. 3D,E). Hematoxylin and Eosin stained sections from wild-type and *Wnt7b^{lacZ-/-}* mice showed that, as expected, the lungs of wild-type mice were properly inflated (Fig. 3F). However, the lungs of *Wnt7b^{lacZ-/-}* mice were not inflated and had a smaller, collapsed appearance (Fig. 3G). *Wnt7b^{lacZ-/-}* mice also exhibited pulmonary hemorrhage, particularly around the large blood vessels (Fig. 3G, Fig. 7H). These results suggest that *Wnt7b^{lacZ-/-}* mice die quickly after birth because of respiratory failure and the lungs of these mice display several notable defects including lung hypoplasia and/or lack of inflation and pulmonary hemorrhage.

Wnt7b^{lacZ-/-} embryos display lung hypoplasia

To further characterize the lung defects in *Wnt7b^{lacZ-/-}* embryos, we examined histological sections from *Wnt7b^{lacZ-/-}* and *Wnt7b^{lacZ+/+}* embryos at E12.5 and E14.5. Both whole-mount and sections from these time points revealed that lung hypoplasia is noticeable as early as E12.5 of development (Fig. 3H-J). Although airway development is largely normal at these time points, a reduced amount of distal mesenchyme, adjacent to the growing epithelial tubules, is observed (Fig. 4A-F). In wild-type lungs this distal mesenchyme is several cell layers thick (Fig. 4A,C,E). However, in *Wnt7b^{lacZ-/-}* embryos, this mesenchyme is extremely thin, sometimes no more than one or two cell layers thick, resulting in the airway tubules forming immediately next to the mesothelium (Fig. 4B,D,F). These observations suggest that growth and/or differentiation of distal lung mesenchyme is affected in *Wnt7b^{lacZ-/-}* embryos.

Table 1. Genotype of *Wnt7b^{lacZ-/-}* mice during embryogenesis and adulthood

Genotype	Age			
	E9.5-E14.5	E16.5-E18.5	P0	Adult
+/+	19	18	18	29
+/-	46	25	35	56
-/-	21	15	17 (dead)	0

To determine whether cell proliferation is affected in *Wnt7b^{lacZ-/-}* embryos, histological sections were stained with a phospho-histone H3 monoclonal antibody to detect cells

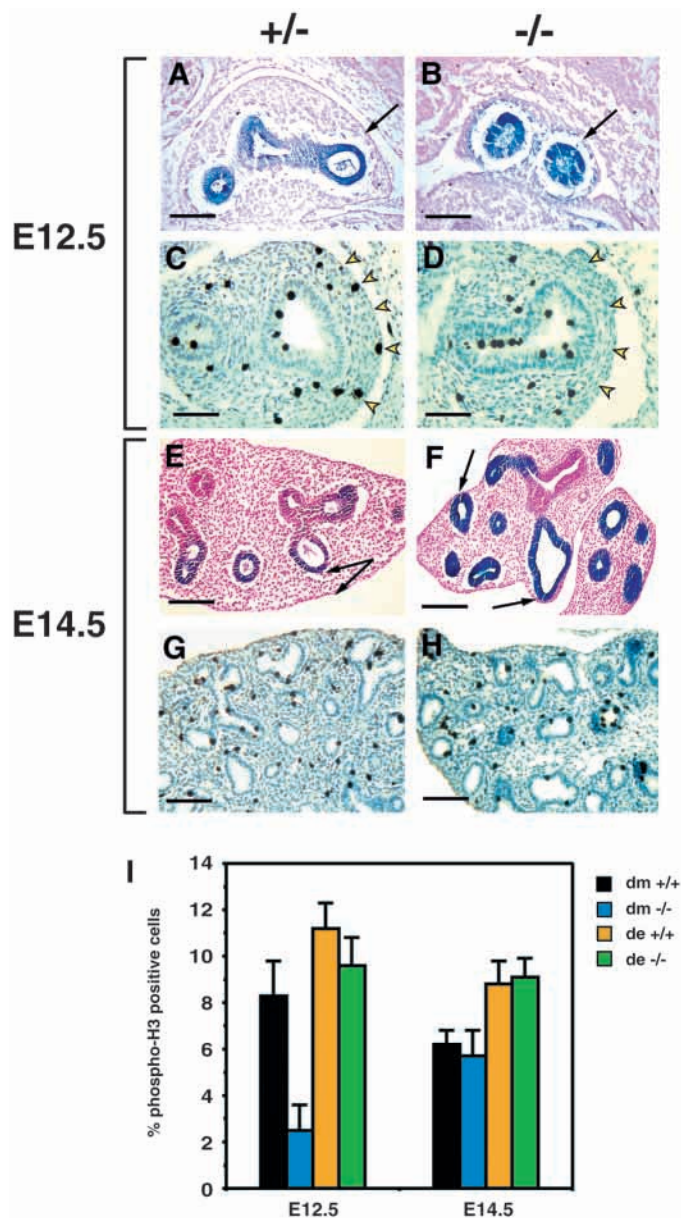


Fig. 4. *Wnt7b^{lacZ-/-}* embryos exhibit thin mesenchyme and reduced distal mesenchyme proliferation at E12.5. *Wnt7b^{lacZ-/-}* embryos at E12.5 and E14.5 exhibit thinner mesenchyme than do *Wnt7b^{lacZ+/+}* littermates, with the airway epithelium growing almost directly next to the mesothelium of the lung (A,B,E,F, arrows). Samples were stained for β -galactosidase expression to better visualize the airway epithelium (A,B,E,F). Staining of lung tissue with a monoclonal antibody to phospho-histone H3, which detects mitotic cells, shows decreased staining in the distal mesenchyme of *Wnt7b^{lacZ-/-}* embryos at E12.5 (C,D, yellow arrowheads). By E14.5, no significant difference in cell proliferation is observed between *Wnt7b^{lacZ-/-}* and *Wnt7b^{lacZ+/+}* embryos in the lung (G,H). Quantification of cell proliferation shows that distal lung mesenchyme proliferation is reduced by approximately two-thirds in E12.5 *Wnt7b^{lacZ-/-}* embryos (I). Scale bars: 150 μ m in A,B; 125 μ m in C,D; 250 μ m in E,F; 200 μ m in G,H. dm, distal mesenchyme; de, distal epithelium.

undergoing mitosis. Quantification of the mitotic cells in the distal mesenchyme of wild-type and *Wnt7b^{lacZ-/-}* embryos shows that proliferation is reduced at E12.5 by approx. two-thirds in *Wnt7b^{lacZ-/-}* embryos (Fig. 4I). By E14.5, this difference in proliferation in the distal mesenchyme between wild-type and *Wnt7b^{lacZ-/-}* embryos was no longer evident (Fig. 4G-I). Furthermore, the number of mitotic airway epithelial cells was unchanged at both E12.5 and E14.5 (Fig. 4C,D,G-I). These data indicate that *Wnt7b* acts as an important mitogen for distal mesenchyme during early lung development.

Differentiation of lung epithelium in *Wnt7b^{lacZ-/-}* embryos

Lung epithelium differentiates during mid to late gestation, resulting in distinct cell lineages along a proximodistal axis (Warburton et al., 2000). To determine whether lung epithelial cell differentiation had occurred properly in *Wnt7b^{lacZ-/-}* embryos, markers for proximal (CC10) and distal (SP-C) epithelial differentiation were used in situ hybridization of E18.5 *Wnt7b^{lacZ-/-}* and wild-type littermates. CC10 expression is normally confined to non-ciliated Clara epithelial cells of the proximal airways, whereas SP-C is expressed exclusively in alveolar type 2 (AEC-2) cells of the distal airways. In situ hybridization reveals that *Wnt7b^{lacZ-/-}* embryos express CC10 and SP-C at normal levels and in a pattern similar to that in wild-type littermates (Fig. 5A-D). These data suggest that proximodistal cell patterning is unaffected in *Wnt7b^{lacZ-/-}* embryos.

From E16.5 through the first 2 weeks after birth, the mouse lung undergoes further differentiation to produce the thin, diffusible surface area used for efficient gas exchange. One of the primary differentiation events that occur during this time is the differentiation of alveolar epithelial type 1 cells (AEC-1), which comprise approximately 95% of the airway surface area and are responsible for gas exchange between blood and air in postnatal animals. Aquaporin 5 encodes a water channel and is expressed in AEC-1 cells in the lung beginning at ~E17.5 (Lee et al., 1997). As previously reported, aquaporin 5 is expressed in the distal airways of the lung at E18.5 (Fig. 5E,F) (Lee et al., 1997; Yang et al., 2002). However, in *Wnt7b^{lacZ-/-}* mice, aquaporin 5 expression is severely attenuated, suggesting that later stages of lung epithelial differentiation are defective (Fig. 5F).

Transmission electron microscopy was performed to verify whether AEC-1 cell differentiation was defective, as suggested by the attenuated aquaporin 5 expression. AEC-1 cells are distinctive in appearance and are characterized by their squamous morphology. The distal airways of E18.5 *Wnt7b^{lacZ-/-}* embryos contained large quantities of cuboidal AEC-2 cells (Fig. 5H, arrowheads). Surfactant is also observed in the airway lumen (Fig. 5H, notice 'S' and arrow). However, almost no AEC-1 cells were observed in *Wnt7b^{lacZ-/-}* lungs, whereas wild-type littermates did contain AEC-1 cells (Fig. 5G, arrow). Together, these results suggest that *Wnt7b^{lacZ-/-}* embryos display a late lung epithelial differentiation/maturation defect that correlates with decreased numbers of AEC-1 cells.

Wnt7b^{lacZ-/-} embryos display pulmonary vascular defects

Wnt7b^{lacZ-/-} mice show hemorrhage surrounding the large pulmonary vessels at birth, suggesting a pulmonary vascular defect in these mice. This hemorrhage is not observed in any

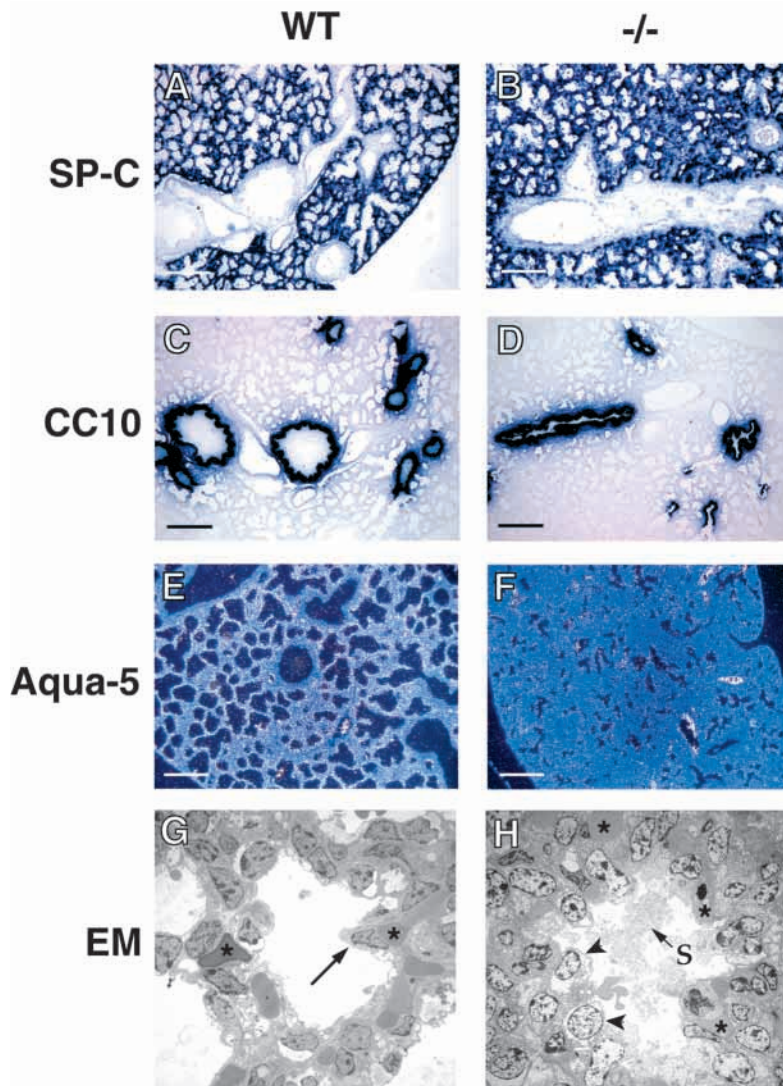


Fig. 5. Lung epithelial cell differentiation marker gene expression in *Wnt7b^{lacZ-/-}* embryos. Sections from E18.5 wild-type and *Wnt7b^{lacZ-/-}* embryos were analyzed by in situ hybridization using probes for SP-C, CC10 and aquaporin 5. The pattern and expression levels of SP-C and CC10 were unchanged in *Wnt7b^{lacZ-/-}* embryos while the level of aquaporin 5 gene expression was reduced in *Wnt7b^{lacZ-/-}* embryos (A-F). Transmission electron microscopy was performed to analyze the morphology of distal airway epithelial cells (G,H). Wild-type lungs tissue revealed both AEC-1 (G, arrow) and AEC-2 cells while *Wnt7b^{lacZ-/-}* lung tissue lacked well defined AEC-1 cells but instead contained only cuboidal AEC-2 cells (H, arrowheads). Both wild-type and *Wnt7b^{lacZ-/-}* lung tissue show an extensive capillary network surrounding the distal airways (G,H asterisks). Scale bars: 250 μ m.

other region of the embryos or neonates, indicating a specific defect in the lung vasculature. Examination of the large blood vessels in the lung at E18.5 shows that many of them are dilated and contain a thickened smooth muscle cell layer (Fig. 6A-D). The number of smooth muscle or endothelial cells does not appear to be increased, suggesting a hypertrophic response and not increased cell proliferation. This is supported by the lack of an increase in phospho-histone H3-positive cells in the pulmonary vasculature of *Wnt7b^{lacZ-/-}* embryos (data not shown). At birth, severe hemorrhage is observed surrounding

the major pulmonary vessels (Fig. 6G,H). This suggests that *Wnt7b^{lacZ-/-}* embryos and mice have dilated and weakened pulmonary vessels that rupture at birth, possibly due to the increased pulmonary blood flow or mechanical strain on the lungs that occurs at birth in association with diaphragm contractions.

To obtain a more thorough picture of blood vessel development in *Wnt7b^{lacZ-/-}* embryos, we injected methacrylate resin into the ventricles of the heart to fill the embryonic vasculature. After the soft tissue of the embryo is digested away, a cast of the cardiovascular system can be visualized (Merscher et al., 2001). As expected, wild-type E18.5 embryos have an extensive pulmonary vascular network with reiterated branching of the large vessels into smaller ones (Fig. 6E). However, in E18.5 *Wnt7b^{lacZ-/-}* embryos, reiterated branching of the smaller pulmonary vessels is reduced (Fig. 6F). In addition, the diameter of the branched vessels is increased, supporting the above histological analysis that indicates dilation of pulmonary blood vessels.

Aberrant smooth muscle α -actin expression and increased cell death in pulmonary vascular smooth muscle of *Wnt7b^{lacZ-/-}* neonates

The dilated blood vessels and hemorrhage observed in the lungs of *Wnt7b^{lacZ-/-}* embryos and neonates suggested possible defects in vascular smooth muscle cell (VSMC) differentiation. To detect whether smooth muscle had differentiated properly in *Wnt7b^{lacZ-/-}* neonates, smooth muscle α -actin immunohistochemistry was performed. In the lung, smooth muscle is normally found surrounding the upper bronchial and tracheal airways and the pulmonary vasculature in late development. Some of the large hemorrhagic blood vessels in *Wnt7b^{lacZ-/-}* neonates contained noticeably less smooth muscle, while most had increased smooth muscle α -actin staining, which was probably due to hypertrophy (Fig. 7E,F). Both types of vessels displayed extensive hemorrhage (Fig. 7E,F). By contrast, bronchial smooth muscle was well formed and observed surrounding all of the large upper airways of both wild-type and *Wnt7b^{lacZ-/-}* neonates (Fig. 7G,H).

TUNEL staining was performed on wild-type and *Wnt7b^{lacZ-/-}* lung tissue to determine whether increased cell death was observed in the pulmonary blood vessels of *Wnt7b^{lacZ-/-}* mice. As shown in Fig. 7J, VSMCs of *Wnt7b^{lacZ-/-}* neonatal mice exhibited extensive TUNEL staining when compared with wild-type littermates (Fig. 7J). This was not observed in bronchial smooth muscle cells (Fig. 7K) or in the vascular smooth muscle of wild-type littermates (Fig. 7I). This data suggests that Wnt7b is important for the differentiation and/or maintenance of pulmonary VSMCs in the lung.

To determine whether the smaller capillaries in the lung, which lack vascular smooth muscle, were affected in *Wnt7b^{lacZ-/-}* embryos, lung tissue from neonatal mice was immunohistochemically stained with an antibody to

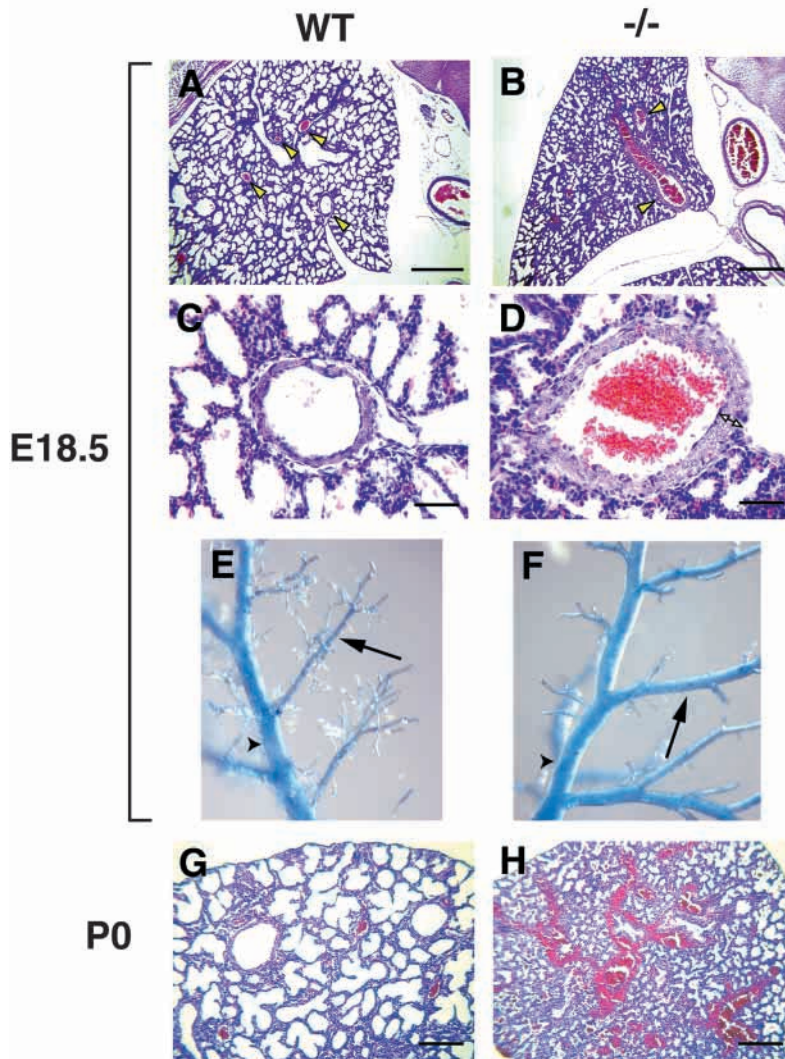


Fig. 6. *Wnt7b^{lacZ-/-}* embryos and neonates exhibit pulmonary hemorrhage due to defects in the vasculature. Analysis of *Wnt7b^{lacZ-/-}* embryos at E18.5 shows dilatation of large blood vessels compared with wild-type littermates (A,B, arrowheads; C,D). The blood vessel wall is also thicker in *Wnt7b^{lacZ-/-}* embryos (D, double-headed arrow). Injection of latex resin to form a cast of the embryonic vasculature reveals that the branched vessels in *Wnt7b^{lacZ-/-}* embryos are larger in diameter and the degree of reiterated branching is reduced (E,F, arrows). However, the main trunk vessel diameter is unchanged in *Wnt7b^{lacZ-/-}* embryos (E,F, arrowheads). At birth, *Wnt7b^{lacZ-/-}* neonates exhibit extensive hemorrhage in the lungs, primarily surrounding the larger blood vessels (G,H). Scale bars: 500 μ m in A,B; 75 μ m in C,D; 250 μ m in G,H.

platelet endothelial adhesion molecule (PECAM). PECAM staining of both wild-type and *Wnt7b^{lacZ-/-}* littermates is normal, with the capillary plexus staining strongly (Fig. 7L,M). This suggests that lung vascular endothelial development in *Wnt7b^{lacZ-/-}* embryos occurs normally. Several blood vessels that exhibited hemorrhage showed rupture of the vascular smooth muscle wall with herniation of the endothelial lining (Fig. 7N). This observation supports the hypothesis that *Wnt7b^{lacZ-/-}* late stage embryos and neonates exhibit vascular smooth muscle-specific defects in the lung, which lead to perinatal hemorrhage in *Wnt7b^{lacZ-/-}* neonates.

DISCUSSION

Signaling molecules originating from the mesenchyme are known to regulate lung development (reviewed by Warburton et al., 2000). Much less is known about putative signals originating from the epithelial cells and how these might affect development of the lung mesenchyme. We demonstrate that a member of the Wnt family, *Wnt7b*, regulates growth and differentiation of lung mesenchyme in mice. *Wnt7b^{lacZ-/-}* embryos and neonates exhibit lung hypoplasia characterized by reduced mesenchymal cell proliferation early in development and, in addition, exhibit a delay in lung epithelial maturation. Later in development, *Wnt7b^{lacZ-/-}* embryos and neonates develop pulmonary VSMC defects, which lead to vessel rupture and hemorrhage at birth. Together, these data demonstrate for the first time a key role for Wnt signaling in lung development.

Wnt7b and lung mesenchymal proliferation

Wnt7b is the only Wnt gene that we have found to be expressed exclusively in the airway epithelium of the lung during early embryonic development. Other Wnt genes, such as *Wnt2*, *Wnt2b* and *Wnt11* are expressed in the mesenchyme of the developing lung (Lako et al., 1998; Lin et al., 2001; Monkley et al., 1996). However, there is no reported lung phenotype in *Wnt2*-null mice, suggesting that any role *Wnt2* may play is rescued through overlapping expression of other Wnt genes such as *Wnt2b* or *Wnt11* (Lako et al., 1998; Lin et al., 2001; Monkley et al., 1996). Our data show that *Wnt7b* plays an essential role in proliferation of the lung mesenchyme. This observation is noticeable early in development in mesenchymal cells directly adjacent to the growing airway epithelium where *Wnt7b* is expressed. However, at E14.5 and later in development, proliferation is not noticeably affected. Interestingly, early mesenchyme differentiation does not appear to be affected in *Wnt7b^{lacZ-/-}* embryos, as demonstrated by normal expression of *Wnt2* and FGF-10 (data not shown). Thus, *Wnt7b* is required for normal lung mesenchymal proliferation in a narrow window of development prior to E14.5.

Regulation of cell proliferation is a key function of Wnt signaling and various members of the Wnt family have been implicated in regulating proliferation in the forming limb, hematopoietic cells, and intestinal and mammary epithelium (Bradley and Brown, 1995; Edwards et al., 1992; Lickert et al., 2000; Morin, 1999; Reya et al., 2000; Van Den Berg et al., 1998; Wong et al., 1998; Yamaguchi et al., 1999). Our data indicate that *Wnt7b* signals derived from the lung epithelium regulate lung mesenchymal proliferation. Regulation of cell proliferation by Wnts involves both the β -catenin canonical pathway as well as through protein kinase C-dependent mechanisms (Morin, 1999; Murray et al., 1999; Wong et al., 1998). Further investigation will be necessary to determine whether *Wnt7b* signals through β -catenin-dependent or -independent pathways during lung development.

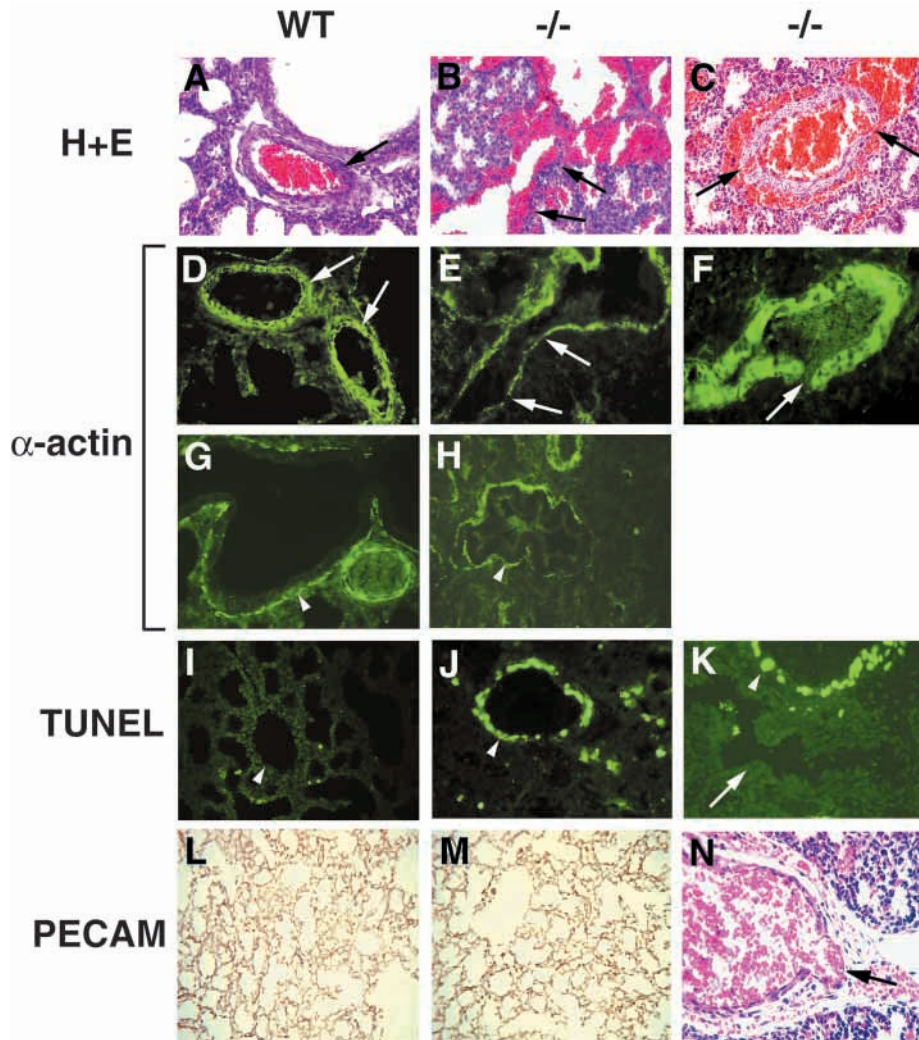


Fig. 7. Defective smooth muscle integrity in *Wnt7b^{lacZ-/-}* embryos and mice. Close examination of blood vessels in wild-type (A, arrow) and *Wnt7b^{lacZ-/-}* P0 neonates (B,C) reveals several breaches in the vessel wall in *Wnt7b^{lacZ-/-}* mice. In some instances, very little of the structure of the wall is left (B, arrows), while in others a thicker vessel wall with several ruptures is observed (C, arrows). Staining of sections with an antibody against smooth muscle α -actin shows robust staining surrounding blood vessels in wild-type neonates (D, arrows). Smooth muscle α -actin staining shows reduced staining, suggesting degradation of smooth muscle surrounding some vessels in *Wnt7b^{lacZ-/-}* neonates (E, arrows), while other vessels show frank breaches in the hypertrophic vessel wall (F). Bronchial smooth muscle appears normal in both wild-type (G, arrowhead) and *Wnt7b^{lacZ-/-}* neonates (H, arrowhead). TUNEL staining shows an increase in TUNEL-positive cells in the smooth muscle of the blood vessel wall in *Wnt7b^{lacZ-/-}* neonates (J, arrowhead) but not in bronchial smooth muscle (K, arrow). This is not observed in wild-type littermates (I, arrow). PECAM staining reveals a normal endothelial network in wild-type (L) and *Wnt7b^{lacZ-/-}* neonates (M). Many large blood vessels showed rupture of the smooth muscle layer with herniation of the intact endothelial cell layer (N, arrow).

SHH and BMP4 also appear to affect cell proliferation in both mesenchymal and epithelial cells of the lung. Overexpression of SHH in the distal airway epithelium of the lung causes increased cell proliferation in both mesenchymal and epithelial cell types (Bellusci et al., 1997). In addition, *Shh*-null mice have a significantly reduced level of cell proliferation in both the mesenchyme and airway epithelium (Litingtung et al., 1998; Pepicelli et al., 1998). Over-expression of BMP4 results in decreased cell proliferation in the epithelium and an increase in the mesenchyme (Bellusci et al., 1996). In *Wnt7b^{lacZ-/-}* embryos, SHH and BMP4 expression do not appear to be affected suggesting that these genes are not regulated by *Wnt7b* signaling (data not shown). In turn, *Wnt7b* expression is not affected in *Shh*-null embryos (Pepicelli et al., 1998). Together, these data suggest that cell proliferation in lung morphogenesis is controlled by several distinct pathways (Fig. 8A).

***Wnt7b* and lung epithelial cell differentiation and maturation**

Wnt7b^{lacZ-/-} embryos exhibit normal proximal-distal epithelial cell differentiation as shown by the expression patterns of SP-C and CC10. This indicates that *Wnt7b* does not regulate this

proximodistal patterning process in airway epithelium in mice. Expression of surfactant by electron microscopy and immunohistochemical staining for surfactant proteins B and C indicates that production of surfactant is not grossly compromised in *Wnt7b^{lacZ-/-}* embryos (Fig. 6 and data not shown). However, *Wnt7b^{lacZ-/-}* embryos exhibit a decrease in expression of the late differentiation marker gene aquaporin 5. Coupled with a decrease in AEC-1 cells in the lungs of *Wnt7b^{lacZ-/-}* embryos, these data suggest that late lung maturation is disrupted in *Wnt7b^{lacZ-/-}* embryos. The differentiation of AEC-2 cells into AEC-1 cells late in lung development is necessary to form the thin, diffusible stratum between the airway lumen and the pulmonary capillary network (reviewed by Warburton et al., 2000). Several other mouse models that have defects in late lung maturation such as epidermal growth factor 1 receptor-null mice, *Cutl1* null mice and lung-specific GATA6 dominant-negative transgenic mice do not exhibit significant hypoplasia, suggesting that maturation and hypoplasia are not necessarily linked during mouse lung development (Ellis et al., 2001; Miettinen et al., 1997; Yang et al., 2002). In addition, many of these mice die quickly after birth because of respiratory failure, supporting the importance of these late maturation events in postnatal

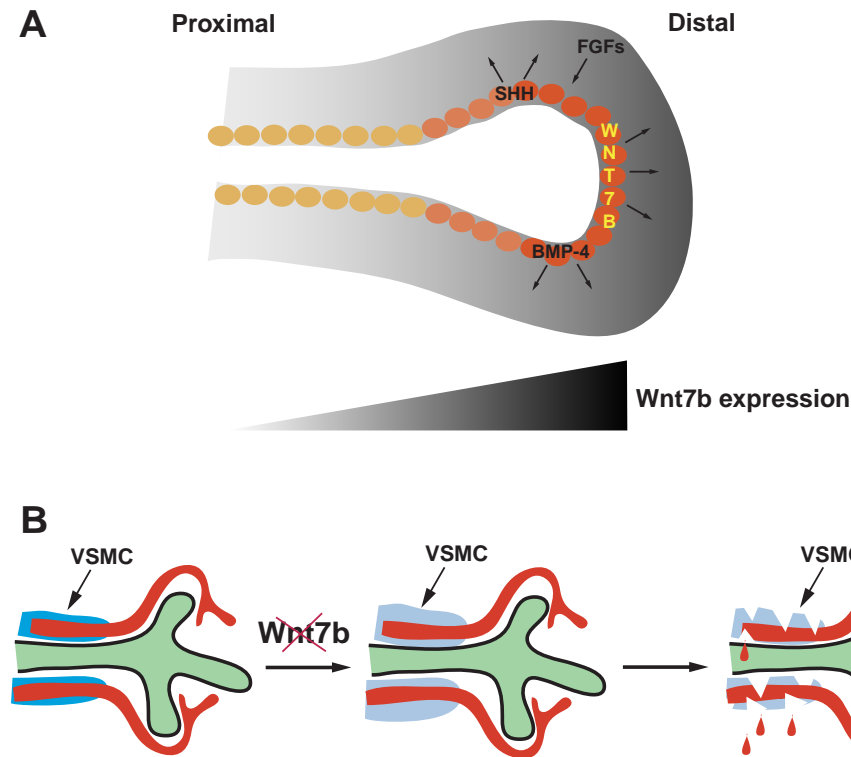


Fig. 8. A model for the role of *Wnt7b* in lung development. (A) *Wnt7b* is expressed at the distal tips of the airway epithelium in a pattern similar to that observed with BMP4 and overlapping that of SHH. In addition, *Wnt7b* is expressed in an increasing gradient from the proximal-to-distal airway epithelium. FGFs are expressed in the mesenchyme and are known to regulate epithelial branching and proliferation. However, because BMP-4 and SHH expression is unchanged in *Wnt7b^{lacZ-/-}* embryos and *Wnt7b* expression is unchanged in *Shh*-null mice, *Wnt7b* regulates mesenchymal proliferation and differentiation through a unique pathway. (B) Lung vasculature is composed of both endothelium (red) and vascular smooth muscle (VSMC, blue), and develops in parallel with the airways (green). Loss of *Wnt7b* function results in defects in vascular smooth muscle differentiation and/or survival leading to a hypertrophic response (change from dark blue to light blue), degradation of the vessel wall and eventual rupture of the weakened vessels.

respiration (Ellis et al., 2001; Miettinen et al., 1997; Yang et al., 2002).

Wnt7b and pulmonary vascular development

Wnt7b^{lacZ-/-} embryos and mice exhibit pulmonary VSMC hypertrophy and apoptosis, suggesting that *Wnt7b* affects late mesenchymal development because smooth muscle in the lung differentiates from the mesenchyme. Because *Wnt7b* is not expressed in vascular smooth muscle cells in the lung, several possibilities exist for the role of *Wnt7b* in vascular development including: (1) it may be required for maintenance of the pulmonary vascular smooth muscle phenotype by acting as a paracrine growth factor; (2) it may be necessary for the expression of other auto- or paracrine factors in mesenchymal or epithelial cell lineages required for VSMC survival; or (3) loss of *Wnt7b* signaling could result in defective differentiation of VSMCs, leading to a block in development and degradation of the smooth muscle component of the vessel wall. The vascular defects in *Wnt7b^{lacZ-/-}* embryos and neonates are unlikely to be linked to lung hypoplasia because other mouse models that have severe lung hypoplasia such as the *Fgf9* knock-out mice exhibit completely normal vascular development (Colvin et al., 2001). Because *Wnt7b* expression decreases during late gestation in the lung (i.e. after E16.5) and is expressed at only low levels in the adult mouse lung (Gavin et al., 1990) (data not shown), *Wnt7b* is likely to play a role during the early events of pulmonary vascular smooth muscle differentiation. Thus, *Wnt7b* may initiate a mesenchymal differentiation program that propagates from the distal to proximal regions as the lung grows, resulting in the proper differentiation of vascular smooth muscle. In this model, as the mesenchyme differentiates and progresses from the distal

towards the proximal region, vascular smooth muscle differentiates and begins to surround the endothelial tubes, establishing the support structure of the large blood vessels in the lung (Fig. 8A,B). Loss of *Wnt7b* function does not result in loss of vascular smooth muscle specification, but does lead to the inability of vascular smooth muscle to maintain its integrity and survive (Fig. 8B). This degradation in the vessel wall could be due to a form of pulmonary hypertension which, in turn, could result in blood vessel wall failure. Thus, inactivation of *Wnt7b* leads to defective smooth muscle differentiation, degradation of the vessel wall, and perinatal hemorrhage.

The observation that vascular smooth muscle but not bronchial smooth muscle is affected in *Wnt7b^{lacZ-/-}* embryos supports a model in which different types of pulmonary smooth muscle are regulated by specific signaling and transcriptional programs. Distinct differences between the molecular programs regulating vascular and visceral smooth muscle development have been identified previously. In particular, transcriptional mechanisms that drive vascular smooth muscle development have been shown to be dependent on the activity of serum response factor, a transcriptional regulator enriched in cardiac and smooth muscle lineages (Kim et al., 1997; Li et al., 1997; Strobeck et al., 2001). The vascular phenotype of *Wnt7b^{lacZ-/-}* embryos provides an important example of the differences in the responses of vascular and bronchial smooth muscle to the Wnt signaling pathway. Interestingly, a recent report implicates the Wnt pathway in the regulation of vascular smooth muscle development (Wang et al., 2002). In particular, β -catenin was elevated in VSMCs from balloon angioplasty-injured aortas, and forced expression of β -catenin increased VSMC proliferation and inhibited apoptosis. These same studies showed that expression of a dominant-negative TCF4

blocked the β -catenin induced inhibition of apoptosis. These data suggest that β -catenin dependent signaling increases cell proliferation and inhibits apoptosis in VSMCs and support the hypothesis that Wnt7b signals through a β -catenin-dependent pathway in pulmonary VSMCs.

The phenotype of *Wnt7b^{lacZ-/-}* mice contrast with those recently reported for another *Wnt7b* mutant, which displays a much earlier defect in amnion and chorion fusion, causing lethality at E10.5 (Parr et al., 2001). Our targeting strategy involved the deletion of the coding sequences of the first exon of *Wnt7b*, while Parr et. al. targeted a region of the third exon (Parr et al., 2001). Although our allele did generate a very low level of transcripts at the 3' end of the gene, the allele generated by Parr et. al. may be expected to produce transcripts from at least the first two exons of *Wnt7b*. As C-terminal truncated Wnts have been used to inhibit Wnt signaling in a dominant-negative manner, a possible explanation for the differences between our results and those of Parr et. al. could be that these authors have generated a dominant-negative allele (Baker et al., 1999; Hoppler et al., 1996; Mullor et al., 2001). Alternatively, the *Wnt7b^{lacZ}* allele might be a hypomorph rather than a true null allele. However, this latter explanation seems unlikely as we deleted the region of the transcript encoding the signal peptide and show that any resulting truncated protein (if generated) is not likely to be stable or secreted, which is supported by previous reports showing that the signal peptide is required for Wnt activity in *Xenopus* embryos and cell culture (Mason et al., 1992; McMahon and Moon, 1989).

In summary, our findings present in vivo evidence that Wnt7b plays a crucial role during lung development, regulating mesenchymal proliferation, late epithelial maturation and pulmonary vascular smooth muscle differentiation and/or survival. Our data demonstrate that signaling from the lung epithelium is necessary for the normal development of lung mesenchyme and demonstrate for the first time that Wnt signals play a key role in this process.

The authors would like to thank Jon Epstein and Sarah Millar for helpful suggestions. We thank Diane Zhou for ES cell injections. This work was supported by grants from the NIH and the AHA to E. E. M.

REFERENCES

- Baker, J. C., Beddington, R. S. and Harland, R. M. (1999). Wnt signaling in *Xenopus* embryos inhibits bmp4 expression and activates neural development. *Genes Dev.* **13**, 3149-3159.
- Ballard, P. L. (1996). Neonatal respiratory disease due to surfactant protein B deficiency. *J. Perinatol.* **16**, S28-S34.
- Bellusci, S., Henderson, R., Winnier, G., Oikawa, T. and Hogan, B. L. (1996). Evidence from normal expression and targeted misexpression that bone morphogenetic protein (Bmp-4) plays a role in mouse embryonic lung morphogenesis. *Development* **122**, 1693-1702.
- Bellusci, S., Furuta, Y., Rush, M. G., Henderson, R., Winnier, G. and Hogan, B. L. (1997). Involvement of Sonic hedgehog (Shh) in mouse embryonic lung growth and morphogenesis. *Development* **124**, 53-63.
- Bradley, R. S. and Brown, A. M. (1995). A soluble form of Wnt-1 protein with mitogenic activity on mammary epithelial cells. *Mol. Cell. Biol.* **15**, 4616-4622.
- Cadigan, K. M. and Nusse, R. (1997). Wnt signaling: a common theme in animal development. *Genes Dev.* **11**, 3286-3305.
- Colvin, J. S., White, A. C., Pratt, S. J. and Ornitz, D. M. (2001). Lung hypoplasia and neonatal death in Fgf9-null mice identify this gene as an essential regulator of lung mesenchyme. *Development* **128**, 2095-2106.
- Edwards, P. A., Hiby, S. E., Papkoff, J. and Bradbury, J. M. (1992). Hyperplasia of mouse mammary epithelium induced by expression of the Wnt-1 (int-1) oncogene in reconstituted mammary gland. *Oncogene* **7**, 2041-2051.
- Ellis, T., Gambardella, L., Horcher, M., Tschanz, S., Capol, J., Bertram, P., Jochum, W., Barrandon, Y. and Busslinger, M. (2001). The transcriptional repressor CDP (Cut1) is essential for epithelial cell differentiation of the lung and the hair follicle. *Genes Dev.* **15**, 2307-2319.
- Evans, M. J., Cabral, L. J., Stephens, R. J. and Freeman, G. (1975). Transformation of alveolar type 2 cells to type 1 cells following exposure to NO₂. *Exp. Mol. Pathol.* **22**, 142-150.
- Gavin, B. J., McMahon, J. A. and McMahon, A. P. (1990). Expression of multiple novel Wnt-1/int-1-related genes during fetal and adult mouse development. *Genes Dev.* **4**, 2319-2332.
- Guyer, B., Hoyert, D. L., Martin, J. A., Ventura, S. J., MacDorman, M. F. and Strobino, D. M. (1999). Annual summary of vital statistics-1998. *Pediatrics* **104**, 1229-1246.
- Hans, F. and Dimitrov, S. (2001). Histone H3 phosphorylation and cell division. *Oncogene* **20**, 3021-3027.
- Hogan, B. L. and Yingling, J. M. (1998). Epithelial/mesenchymal interactions and branching morphogenesis of the lung. *Curr. Opin. Genet. Dev.* **8**, 481-486.
- Hollyday, M., McMahon, J. A. and McMahon, A. P. (1995). Wnt expression patterns in chick embryo nervous system. *Mech. Dev.* **52**, 9-25.
- Hoppler, S., Brown, J. D. and Moon, R. T. (1996). Expression of a dominant-negative Wnt blocks induction of MyoD in *Xenopus* embryos. *Genes Dev.* **10**, 2805-2817.
- Kim, S., Ip, H. S., Lu, M. M., Clendenin, C. and Parmacek, M. S. (1997). A serum response factor-dependent transcriptional regulatory program identifies distinct smooth muscle cell sublineages. *Mol. Cell. Biol.* **17**, 2266-2278.
- Kuo, C. T., Morrisey, E. E., Anandappa, R., Sigrist, K., Lu, M. M., Parmacek, M. S., Soudais, C. and Leiden, J. M. (1997). GATA4 transcription factor is required for ventral morphogenesis and heart tube formation. *Genes Dev.* **11**, 1048-1060.
- Lako, M., Strachan, T., Bullen, P., Wilson, D. I., Robson, S. C. and Lindsay, S. (1998). Isolation, characterisation and embryonic expression of WNT11, a gene which maps to 11q13.5 and has possible roles in the development of skeleton, kidney and lung. *Gene* **219**, 101-110.
- Lee, M. D., King, L. S., Nielsen, S. and Agre, P. (1997). Genomic organization and developmental expression of aquaporin-5 in lung. *Chest* **111**, 111S-113S.
- Li, L., Liu, Z., Mercer, B., Overbeek, P. and Olson, E. N. (1997). Evidence for serum response factor-mediated regulatory networks governing SM22alpha transcription in smooth, skeletal, and cardiac muscle cells. *Dev. Biol.* **187**, 311-321.
- Lickert, H., Domon, C., Huls, G., Wehrle, C., Duluc, I., Clevers, H., Meyer, B. I., Freund, J. N. and Kemler, R. (2000). Wnt/(beta)-catenin signaling regulates the expression of the homeobox gene Cdx1 in embryonic intestine. *Development* **127**, 3805-3813.
- Lin, Y., Liu, A., Zhang, S., Ruusunen, T., Kreidberg, J. A., Peltoketo, H., Drummond, I. and Vainio, S. (2001). Induction of ureter branching as a response to Wnt-2b signaling during early kidney organogenesis. *Dev. Dyn.* **222**, 26-39.
- Lippincott-Schwartz, J., Bonifacino, J. S., Yuan, L. C. and Klausner, R. D. (1988). Degradation from the endoplasmic reticulum: disposing of newly synthesized proteins. *Cell* **54**, 209-220.
- Litingtung, Y., Lei, L., Westphal, H. and Chiang, C. (1998). Sonic hedgehog is essential to foregut development. *Nat. Genet.* **20**, 58-61.
- Lu, M. M., Yang, H., Zhang, L., Shu, W., Blair, D. G. and Morrisey, E. E. (2001). The bone morphogenic protein antagonist gremlin regulates proximal-distal patterning of the lung. *Dev. Dyn.* **222**, 667-680.
- Mason, J. O., Kitajewski, J. and Varmus, H. E. (1992). Mutational analysis of mouse Wnt-1 identifies two temperature-sensitive alleles and attributes of Wnt-1 protein essential for transformation of a mammary cell line. *Mol. Biol. Cell* **3**, 521-533.
- McMahon, A. P. and Moon, R. T. (1989). Ectopic expression of the proto-oncogene int-1 in *Xenopus* embryos leads to duplication of the embryonic axis. *Cell* **58**, 1075-1084.
- Merscher, S., Funke, B., Epstein, J. A., Heyer, J., Puech, A., Lu, M. M., Xavier, R. J., Demay, M. B., Russell, R. G., Factor, S. et al. (2001). TBX1 is responsible for cardiovascular defects in velo-cardio-facial/DiGeorge syndrome. *Cell* **104**, 619-629.
- Miettinen, P. J., Warburton, D., Bu, D., Zhao, J. S., Berger, J. E., Minoo,

- P., Koivisto, T., Allen, L., Dobbs, L., Werb, Z. et al.** (1997). Impaired lung branching morphogenesis in the absence of functional EGF receptor. *Dev. Biol.* **186**, 224-236.
- Monkley, S. J., Delaney, S. J., Pennisi, D. J., Christiansen, J. H. and Wainwright, B. J.** (1996). Targeted disruption of the Wnt2 gene results in placental defects. *Development* **122**, 3343-3353.
- Morin, P. J.** (1999). beta-catenin signaling and cancer. *BioEssays* **21**, 1021-1030.
- Mullor, J. L., Dahmane, N., Sun, T. and Ruiz i Altaba, A.** (2001). Wnt signals are targets and mediators of Gli function. *Curr. Biol.* **11**, 769-773.
- Murray, N. R., Davidson, L. A., Chapkin, R. S., Clay Gustafson, W., Schattenberg, D. G. and Fields, A. P.** (1999). Overexpression of protein kinase C betaII induces colonic hyperproliferation and increased sensitivity to colon carcinogenesis. *J. Cell Biol.* **145**, 699-711.
- Nielsen, H., Engelbrecht, J., Brunak, S. and von Heijne, G.** (1997). Identification of prokaryotic and eukaryotic signal peptides and prediction of their cleavage sites. *Protein Eng.* **10**, 1-6.
- Nogee, L. M., Garnier, G., Dietz, H. C., Singer, L., Murphy, A. M., deMello, D. E. and Colten, H. R.** (1994). A mutation in the surfactant protein B gene responsible for fatal neonatal respiratory disease in multiple kindreds. *J. Clin. Invest.* **93**, 1860-1863.
- Parr, B. A., Cornish, V. A., Cybulsky, M. I. and McMahon, A. P.** (2001). Wnt7b regulates placental development in mice. *Dev. Biol.* **237**, 324-332.
- Parr, B. A. and McMahon, A. P.** (1994). Wnt genes and vertebrate development. *Curr. Opin. Genet. Dev.* **4**, 523-528.
- Parr, B. A., Shea, M. J., Vassileva, G. and McMahon, A. P.** (1993). Mouse Wnt genes exhibit discrete domains of expression in the early embryonic CNS and limb buds. *Development* **119**, 247-261.
- Pepicelli, C. V., Lewis, P. M. and McMahon, A. P.** (1998). Sonic hedgehog regulates branching morphogenesis in the mammalian lung. *Curr Biol* **8**, 1083-1086.
- Reya, T., O'Riordan, M., Okamura, R., Devaney, E., Willert, K., Nusse, R. and Grosschedl, R.** (2000). Wnt signaling regulates B lymphocyte proliferation through a LEF-1 dependent mechanism. *Immunity* **13**, 15-24.
- Rubenstein, J. L., Anderson, S., Shi, L., Miyashita-Lin, E., Bulfone, A. and Hevner, R.** (1999). Genetic control of cortical regionalization and connectivity. *Cereb. Cortex* **9**, 524-532.
- Saka, Y. and Smith, J. C.** (2001). Spatial and temporal patterns of cell division during early *Xenopus* embryogenesis. *Dev. Biol.* **229**, 307-318.
- Strobeck, M., Kim, S., Zhang, J. C., Clendenin, C., Du, K. L. and Parmacek, M. S.** (2001). Binding of serum response factor to CARG box sequences is necessary but not sufficient to restrict gene expression to arterial smooth muscle cells. *J. Biol. Chem.* **276**, 16418-16424.
- Van den Berg, D. J., Sharma, A. K., Bruno, E. and Hoffman, R.** (1998). Role of members of the Wnt gene family in human hematopoiesis. *Blood* **92**, 3189-3202.
- Wang, X., Xiao, Y., Mou, Y., Zhao, Y., Blankesteyn, W. M. and Hall, J. L.** (2002). A role for the beta-catenin/T-cell factor signaling cascade in vascular remodeling. *Circ. Res.* **90**, 340-347.
- Warburton, D., Schwarz, M., Tefft, D., Flores-Delgado, G., Anderson, K. D. and Cardoso, W. V.** (2000). The molecular basis of lung morphogenesis. *Mech. Dev.* **92**, 55-81.
- Weaver, M., Yingling, J. M., Dunn, N. R., Bellusci, S. and Hogan, B. L.** (1999). Bmp signaling regulates proximal-distal differentiation of endoderm in mouse lung development. *Development* **126**, 4005-4015.
- Weidenfeld, J., Shu, W., Zhang, L., Millar, S. E. and Morrisey, E. E.** (2002). The WNT7B Promoter is Regulated by TTF-1, GATA6, and Foxa2 in Lung Epithelium. *J. Biol. Chem.* (in press).
- Willert, K. and Nusse, R.** (1998). Beta-catenin: a key mediator of Wnt signaling. *Curr. Opin. Genet. Dev.* **8**, 95-102.
- Wodarz, A. and Nusse, R.** (1998). Mechanisms of Wnt signaling in development. *Annu. Rev. Cell Dev. Biol.* **14**, 59-88.
- Wong, M. H., Rubinfeld, B. and Gordon, J. I.** (1998). Effects of forced expression of an NH2-terminal truncated beta-Catenin on mouse intestinal epithelial homeostasis. *J. Cell Biol.* **141**, 765-777.
- Yamaguchi, T. P., Bradley, A., McMahon, A. P. and Jones, S.** (1999). A Wnt5a pathway underlies outgrowth of multiple structures in the vertebrate embryo. *Development* **126**, 1211-1223.
- Yang, H., Lu, M. M., Zhang, L., Whitsett, J. A. and Morrisey, E. E.** (2002). GATA6 regulates differentiation of distal lung epithelium. *Development* **129**, (in press).
- Zhang, J. C., Kim, S., Helmke, B. P., Yu, W. W., Du, K. L., Lu, M. M., Strobeck, M., Yu, Q. and Parmacek, M. S.** (2001). Analysis of SM22alpha-deficient mice reveals unanticipated insights into smooth muscle cell differentiation and function. *Mol. Cell Biol.* **21**, 1336-1344.